Intra-parotid facial nerve path by MRI tractography: radio-clinical comparison in parotid tumors

Axelle Thierry, Coralie Barbe, Marc Labrousse, Marc Makeieff, Jean-Claude Merol, Aline Carsin-Vu, France Truong, Xavier Dubernard, Esteban Brenet

European Archives of Oto-Rhino-Laryngology

INTRA-PAROTID FACIAL NERVE PATH BY MRI TRACTOGRAPHY, RADIO-CLINICAL COMPARISON IN PAROTID TUMOURS

--Manuscript Draft--

Manuscript Number:	EAOR-D-23-01180R3
Full Title:	INTRA-PAROTID FACIAL NERVE PATH BY MRI TRACTOGRAPHY, RADIO-CLINICAL COMPARISON IN PAROTID TUMOURS
Article Type:	Head & Neck (Original Article)
Keywords:	Intraparotid facial nerve; Intraparotid mass; MRI tractography; surgery; Concordance
Corresponding Author:	Esteban Brenet, MD, PhD CHU Reims: Centre Hospitalier Universitaire de Reims Reims, Marne FRANCE
Corresponding Author Secondary Information:	
Corresponding Author's Institution:	CHU Reims: Centre Hospitalier Universitaire de Reims
Corresponding Author's Secondary Institution:	
First Author:	Axelle Thiery, MD
First Author Secondary Information:	
Order of Authors:	Axelle Thiery, MD
	Coralie Barbe, MD, PhD
	Marc Labrousse, MD, PhD
	Jean-Claude Mérol, MD
	Marc Makeieff, MD, PhD
	Aline Carsin-Vu, MD
	France Truong, MD
	Xavier Dubernard, MD, PhD
	Esteban Brenet, MD, PhD
Order of Authors Secondary Information:	
Funding Information:	
Abstract:	Purpose: The objective of our study was to evaluate the ability of preoperative MRI tractography to visualize and predict the path of the facial nerve with respect to an intraparotid mass. Methods: We performed an observational bicentric study from June 2019 to August 2020. All patients older than 18 years old, treated for a parotid mass with surgical indication, without MRI contraindication and who agreed to participate in the study were enrolled prospectively. All patients underwent a cervicofacial MRI with tractographic analysis. Postprocessed tractography images of the intraparotid facial nerve were analysed by two expert radiologists in head and neck imaging. The intraoperative anatomical description of the facial nerve path and its relationship to the mass was performed by the surgeon during the operation, with no visibility on MRI examination results. A statistical study allowed for the description of the data collected as well as the measurement of interobserver agreement and agreement between tractography and surgery using kappa coefficients. Results: Fifty-two patients were included. The facial nerve trunk and its first two divisional branches were visualized via tractography in 93.5% of cases (n=43). The upper distal branches were visualized in 51.1% of cases (n=23), and the lower branches were visualized in 73.3% of cases (n=33). Agreement with the location

	described per-operatively was on average 82.9% for the trunk, 74.15% for the temporal branch, and 75.21% for the cervico-facial branch. Conclusion: Fibre tractography analysis by MRI of the intraparotid facial nerve appears to be a good test for predicting the path of the nerve over the parotid mass and could be an additional tool to guide the surgeon in the operative procedure.

October 6th, 2023

Corresponding author:
Dr Esteban Brenet
Robert Debré University Hospital Center
Rue du Général Koenig
51100 Reims (France)
Mail: ebrenet@chu-reims.fr
Phone number: 00-33-0326783781 / 00-33-0670460186

To: The Editorial Board of European Archives of Oto-Rhino-Laryngology (response 3rd round)

Dear reviewers, dear editors,

The authors would particularly like to thank the 2 reviewers who took time to read again the article and to suggest corrections or details that allow a better understanding of our study and a better development of the results.

The authors have tried to respond as best they can, point by point, to the different questions of the reviewers and hope that the details will be sufficient to be accepted in your review.

Below is the point-by-point response to reviewer's comments by color code: black: 3rd round reviewers' comments

Red with big police: author's responses

Each modification was added to the text, Figures and Tables, in red. The manuscript, with all figures and tables, has been sent to an accredited organization (Springer Nature) for full English proofreading.

The authors are at the disposal of the reviewers for any further clarifications they consider necessary.

Yours sincerely,

Dr Esteban Brenet on behalf of the authors.

REVIEW REPORT EAOR-D-23-01180

Responses to AUTHORS (third round)

Reviewer #1: The authors did the changes asked by the reviewer and did respond to all questions.

Reviewer #2: Dear authors
Thank you for taking the recommendations into account. There are only two small details missing that still need to be corrected.

M&M: BLADE abbreviation, misses
Thank you for this clarification. After some research, "BLADE" corresponds to a specific sequence of a brand name (Siemens T2). To avoid this and keep the generic name, we suggest changing "BLADE" to "PROPELER (Periodically Rotated Overlapping ParallEl Lines with Enhanced Reconstruction ».

Discussion: Page 9, second paragraph: again, change post-treatment
It is done

INTRA-PAROTID FACIAL NERVE PATH BY MRI TRACTOGRAPHY, RADIO-CLINICAL COMPARISON IN PAROTID TUMOURS

Axelle THIERRY[1,2] MD, Coralie BARBE[3] MD-PhD, Marc LABROUSSE[1,2] MD-PhD, Marc MAKEIEFF[1,2] MD-PhD, Jean-Claude MEROL[1] MD, Aline CARSIN-VU[3] MD, France TRUONG[1,2], Xavier DUBERNARD[1,2] MD-PhD, Esteban BRENET,[1,2] MD-PhD*

[1] Department of oto-rhino-laryngology, head and neck surgery, University hospital of Reims, France

[2] University of Reims-Champagne Ardennes, France

[3] University Department of Health Research, University of Reims Champagne Ardennes, France

[4] Department or Radiology, University hospital of Reims, France

* Corresponding author: Esteban Brenet, Department of oto-rhino-laryngology, head and neck surgery, University hospital of Reims, France.
ebrenet@chu-reims.fr

ABSTRACT

Purpose: The objective of our study was to evaluate the ability of preoperative MRI tractography to visualize and predict the path of the facial nerve with respect to an intraparotid mass.

Methods: We performed an observational bicentric study from June 2019 to August 2020. All patients older than 18 years old, treated for a parotid mass with surgical indication, without MRI contraindication and who agreed to participate in the study were enrolled prospectively. All patients underwent a cervicofacial MRI with tractographic analysis. Postprocessed tractography images of the intraparotid facial nerve were analysed by two expert radiologists in head and neck imaging. The intraoperative anatomical description of the facial nerve path and its relationship to the mass was performed by the surgeon during the operation, with no visibility on MRI examination results. A statistical study allowed for the description of the data collected as well as the measurement of interobserver agreement and agreement between tractography and surgery using kappa coefficients.

Results: Fifty-two patients were included. The facial nerve trunk and its first two divisional branches were visualized via tractography in 93.5% of cases (n=43). The upper distal branches were visualized in 51.1% of cases (n=23), and the lower branches were visualized in 73.3% of cases (n=33). Agreement with the location described per-operatively was on average 82.9% for the trunk, 74.15% for the temporal branch, and 75.21% for the cervico-facial branch.
Conclusion: Fibre tractography analysis by MRI of the intraparotid facial nerve appears to be a good test for predicting the path of the nerve over the parotid mass and could be an additional tool to guide the surgeon in the operative procedure.

Keywords:
Intraparotid facial nerve; Intraparotid mass; MRI tractography; Surgery; Concordance

INTRA-PAROTID FACIAL NERVE PATH BY MRI TRACTOGRAPHY, RADIO-CLINICAL COMPARISON IN PAROTID TUMOURS

ABSTRACT

Purpose: The objective of our study was to evaluate the ability of preoperative MRI tractography to visualise and predict the path of the facial nerve with respect to an intra-parotid mass.

Methods: We performed an observational bicentric study from June 2019 to August 2020. All patients older than 18 years old, treated for a parotid mass with surgical indication, without MRI contraindication and who agreed to participate in the study were enrolled prospectively. All patients underwent a cervicofacial MRI with tractographic analysis. Post-processed images of the tractography of the intraparotid facial nerve were analyzed by two expert radiologists in head and neck imaging. The intraoperative anatomical description of the facial nerve path and its relationship to the mass was performed by the surgeon during the operation, with no visibility on MRI examination results. A statistical study allowed the description of the data collected as well as the measurement of inter-observer agreement and agreement between tractography and surgery using Kappa coefficients.

Results: 52 patients were included. The facial nerve trunk and its first two divisional branches were visualized via tractography in 93.5% of cases (n=43). The upper distal branches were visualized in 51.1% of cases (n=23) and the lower branches in 73.3% of cases (n=33). Agreement with the location described per-operatively was on average 82.9% for the trunk, 74.15% for the temporal branch, and 75.21% for the cervico-facial branch.

Conclusion: Fiber tractography analysis by MRI of the intraparotid facial nerve appears to be a good test for predicting the path of the nerve over the parotid mass and could be an additional tool to guide the surgeon in the operative procedure.

Ethical statement : the authors declare no conflict of interest.

INTRODUCTION

Parotid lesions account for 3% of tumors of the head and neck and 80% of tumors of the salivary glands(1). They affect mostly adults, and are benign in 80% of cases (2). Surgical removal of this gland, the gold standard treatment (3)(4) called parotidectomy, is complex and presents a major risk for the facial nerve. Indeed, it makes its way through the gland, dividing initially into 2 branches, a temporal branch and a cervico-facial branch, which also divide in a variable manner into several terminal branches, innervating the muscles responsible for facial motion: the frontal, orbicular of the eye, and zygomatic branches coming from the temporal branch and the orbicular branches of the mouth, mandibular, and cervical branches coming from the cervico-facial branch (5).

Surgery consists of exposing the trunk and then dissecting each branch in order to elevate the superficial lobe covering it, sometimes completed by the removal of the deep lobe (6). A key focus point is the preservation of this nerve in order to avoid iatrogenic peripheral facial paralysis.

Preoperative analysis of the intra parotid facial nerve pathway is not used in current practice. Several procedures have been described, using MRI with a gradient of 3 Tesla : anatomical 3D sequences, with positive contrast of the facial nerve using double water excitation and negative contrast, and tractography analysis using Diffusion MRI (7).

Tractography was first described to visualize white matter bundles on the central nervous system (8) and then for large peripheral nerves such as the sciatic or median nerves (9). It is also used preoperatively in ponto-cerebellar angle surgeries to locate the facial nerve(10).

Regarding the intraparotid facial nerve, tractography has been proposed to predict the contact of parotid tumors with the facial nerve preoperatively without specifying the exact topography of its path or the infiltration by malignant tumors (14) and to validate the reliability of the technique by comparing the path in imaging with that found by dissection on cadaver (12).

The main objective of the study was to evaluate the radio-clinical association of the facial nerve path in relation to a parotid lesion by comparing the path obtained by MRI tractography preoperatively to that encountered by the surgeon intraoperatively.

MATERIALS AND METHODS

PATIENTS

An observational bicentric study was performed from June 2019 to August 2020. All patients older than 18 years old, treated in two reference centers for a parotid mass with surgical indication, without MRI contraindication and who agreed to participate in the study were enrolled prospectively.

This study was approved by the Ethics Committee (CPP Nord-Ouest II, Amiens, June 13, 2019) and registered in clinicaltrials.gov (NCT03950323; May 15, 2019). Every patient provided an informed written consent.

OUTCOMES OF THE STUDY AND DATA COLLECTION

For each patient, baseline patient's characteristics (age, sex, diabetes mellitus) and baseline tumor's characteristics (location, size) were recorded.

The Diffusion MRI sequence necessary for the tractography was added to the protocol routinely performed for the diagnostic, extending the duration of the MRI examination by 9 minutes. Central image review of tractography was conducted by two head and neck experienced radiologists and then reported the findings on a standardized questionnaire. The surgical procedure was not affected by the patient's participation in the study. The surgeon recorded the intra parotid facial nerve pathway and its relationship to the tumor mass on the same standardized questionnaire as that of the radiologists without information concerning the tractography's results.

Magnetic Resonance Imaging (MRI) ACQUISITIONS

All examinations were performed on the same Siemens Skyra ® 3.0Tesla MRI with a 64-element head-neck antenna. The following sequences were added to the standard protocol (T1 Turbo Spin Echo (T1TSE) pre- and post-contrast, T2 coronal and axial PROPELER (Periodically Rotated Overlapping ParallEl Lines with Enhanced Reconstruction), and 3D T1 Volumetric Interpolated Breath-hold Examination (VIBE).

The parameters of the diffusion sequence were as follows: repetition time (TR): 3900 ms, Echo time (TE): 90 ms, b-value of 1000 s / mm2, 60 directions acquired voxel size: 2 mm^3, field of view (FOV): 1960 mm, simultaneous multislice acquisitions (SMS), as well as spin echo sequence with 67 slices, number of signal averages of 2, and scan time 4 minutes and 42 seconds. This sequence was acquired a second time with phase encoding inversion to correct

geometric distortion induced by field inhomogeneity B0 (13): antero-posterior and postero-anterior sequences with the topup and eddy commands of the FSL5® software (https://fsl.fmrib.ox.ac.uk/fsl/fslwiki), as integrated in the freeware MRtrix (http://www.mrtrix.org) using the dwifslpreproc function.
The post-processing steps were carried out using the MRtrix software and the MRtrix 3tissues package (14).

Post-processing:
Generation of a distortion-corrected fractional anisotropy (FA) map from tensor values and an estimation of the fiber orientation, distribution using the CSD model (for Constrained Spherical Deconvolution, value of the spherical harmonic coefficient of 6).
Construction of a track-weighted imaging (TWI) map: Generation of 5 million fibers in the entire volume of acquired data using 10 mm as the minimum length for the terminal fibers converted into a TWI map where the value of each voxel represents the average path length (AP) of the fibers passing through the voxel (15).

Local reconstruction of intra-parotid facial nerve fibers (Figure 1):
As described by Attyé et. al (11) the TWI diffusion map was superposed on the T2 anatomical sequence. A first ROI was placed on the Foramen stylomastoidian pulling the fibers with a fixed radius of 3 mm and a number of iterative fibers of 5,000. A second ROI was placed consecutively on the cervico-facial branch and then on the temporal branch in order to pull the fibers from these different branches with a radius fixed at 2mm and a total of 5,000 fibers. The different images obtained were added together to obtain the so-called "most probable" path of the facial nerve within the parotid gland, providing topographical information on its position with respect to the tumor.
When tracking did not allow the branches to be visualized in order to obtain distal information, a plane passing through the first branches of division was modelled in order to predict the division plane of the nerve and its likely position with respect to the mass. Two radiologists did the interpretation of these tractographies and inter-observer agreement was achieved. In the event of disagreement between the two radiologists, the results giving rise to the disagreement were discussed between the two radiologists until agreement was reached.

STATISTICAL ANALYSIS

Qualitative variables were described as number and percentage where quantitative variables were as mean and standard deviation. Interobserver agreement between MRI and surgery were measured using Kappa coefficients, with k values of 0.00–0.20 indicating poor, 0.21– 0.40 indicating fair, 0.41–0.60 indicating moderate, 0.61–0.80 indicating good and 0.81–1.00 indicating excellent interobserver agreement. All analyses were performed using SAS version 9.4 (SAS Institute Inc., Cary, NC, USA).

RESULTS

The flow chart of the study is detailed in Figure 2. 52 patients were prospectively included between June 2019 and August 2020. MRI tractography could be performed in 51 patients. Forty-six patients were operated: 5 patients were not operated due to anesthetic contraindications (n=3) or voluntary withdrawal of the patient from the study (n=2). Three examinations were uninterpretable because of susceptibility artifacts.

Patient characteristics are detailed in Table 1. The mean age at inclusion was 56 years. Four patients had already have a homolateral parotid surgery so were in a revision surgery situation.

Table 2 details the histological characteristics of the tumors and the type of surgery performed. Benign tumors were more frequent than malignant tumors (88% versus 22%).

Table 3 summarizes i) The facial nerve path's tractographic description with respect to the mass: this part reflects the results of the radiological description, which coincided in most cases between the 2 radiologists, with the exception of 3 cases, in which a consensus was previously reached. Disagreement between the two radiologists was discussed in 3 cases involving distal branches, and agreement was finally reached. This discussion took place prior to surgery., ii) the intraoperative facial nerve's surgical description by the surgeon and iii) the concordance between radiologists and surgeon observations.

Visualization of the facial nerve:

The facial nerve trunk and its first two branches of division were visualized in tractography in 93.5% of cases (n=43). The upper distal branches (forehead and eye's branch) were visualized in 51.1% of cases (n=23) and the lower branches (mouth and mandibular) in 73.3% of cases (n=33). The type of division (bifurcation or trifurcation) was not determined by tractography.

Topography of the facial nerve:

The position of the different branches in relation to the tumor evaluated by tractography was concordant with the position described during surgery in 82.9% of cases for the trunk; 74.15% for the temporal branch and 75.21% of cases for the cervico-facial (CF) branch. For the frontal, orbicular of the eyes, orbicular of the mouth and mandibular, the concordance with the actual path was 70%, 74.8%, 76% and 75.4% respectively.

Distance of the facial nerve from the parotid mass:

The distance between the facial nerve and the mass was defined as "far" if assessed at more than 1 centimeter and "near" if assessed at less than 1 centimeter, contact or transfixiant. The radiological assessment was concordant with surgical reality in 85% of cases for the trunk; 84.5% for the temporal branch and 75% of cases for the CF branch. For the frontal, orbicular of the eyes, orbicular of the mouth and mandibular, the concordance was respectively 85.7%, 86.36%, 72.41% and 60%.

Facial nerve routing plane:

The modelling plane passing through the first two divisional branches enables to predict the position of the tumor (outside versus inside) in relation to this plane in 85% of cases. The tumor proximity (more or less than 1 centimeter) from the plane was concordant in 77.5% of cases.

The inter-observer reproducibility between radiologists and surgeon findings was 0.45 for the trunk position with respect to the tumor, 0.47 for the temporal branch, 0.62 for the CF branch and 0.45 for the 4 distal branches combined. The estimated distance between the plane and the tumor has an estimated reproducibility of 0.69 CI 95% [0.43; 0.94].

DISCUSSION

Our study showed that intra-parotid facial nerve tractography prior to parotidectomy enabled to visualize the nerve and the first two division's branches in 93.5% of cases. For the trunk and the first 2 branches, it was matching the real nerve path in 75% of cases and concluded to a contact or proximity reliably in 80% of cases.

To our knowledge, our work is the first prospectively ascertained study which analyses the facial nerve path with respect to a parotid mass with preoperative tractography. The results show acceptable reliability and reproducibility. This examination could be used routinely, as the additional acquisition time required to perform it is acceptable, and the sequences could easily be added to the diagnostic protocol for parotid masses provided that a 3 Tesla MRI and trained technicians for post-processing are available. However, it is important to note that the post-processing work to obtain the tractography is difficult to automate and standardize.

As in previous studies, we found a low sensitivity for the visualization of distal branches of the facial nerve (16)(12), visualized in our study in only 30% of cases out of which it was real path in 70% of cases. Distal branches of the facial nerve being of very small diameter, the MRI signal is too low to image them correctly.

Nevertheless, the virtual construction of the divisional plane allowed us to effectively predict the probable path of the nerve over the mass.

In addition to prejudging contact or not with the tumor as described by Attyé et al. (16), our study shows that tractography analysis is a good approach to map the nerve path and its relationship to the parotid mass, which is an essential information for the surgeon. On the other hand, we did not try to show any signal modification in case of nerve invasion by the tumor as Rouchy et al. found: our series showed perineural damage on final histological examination in only 10% (n=5) of the cases ((14).

A recent study compared the nerve path by tractography with the real path found on 2 cadavers dissection, and finds an exact agreement to the nearest millimeter (12). The advantage of the cadaver is the total immobility and the possibility to test a large number of sequences until the optimal sequence is found. It is acknowledged that an increase of b value decreases the signal-to-noise ratio, requiring acquisition with more direction to avoid signal loss(17). A value of b at 400 mm/s^2 with gradient acquisition in 61 directions allowed them to increase the value of the signal-to-noise and avoid signal loss, thus pulling the nerve more distally, at the expense of

biological significance which is lower since such low values of b mix perfusion and diffusion information.

We made a compromise by performing acquisitions with a b-value of 1000 in 60 directions, allowing a better angular resolution than Attyé et al. and also a better detection rate of distal fibers by keeping an optimal signal-to-noise ratio and reducing motion artifacts. The difficulty of our study is also a likely modification of the signal when the nerve is in contact with the tumor, but this is a better reflection of the clinical application.

As the intra parotid facial nerve cannot be individualized on conventional MRI sequences(7), several techniques have already been studied. The double echo technique with water excitation allows the facial nerve trunk and the cervico-facial branch to be visualized in 100% and 96% of cases respectively and requires few post-treatment. However, this sequence with rapid low-angle shooting is very susceptible to movement artefacts, and therefore has difficulty distinguishing the nerve from the salivary ducts and vessels, and does not always visualize the temporal-facial branch, as its direction forms too sharp angle with the trunk. Moreover, it is not adapted to the description of tumors, requiring in practice a classical diagnostic acquisition in addition to this sequence (18).

MRI negative contrast neurography sequence uses very fine anatomical sequences in order to follow the nerve section by section. Imaging of the extracranial facial nerve with three-dimensional variable flip angle turbo spin echo (VFA-TSE) depicts the nerve as a low signal structure (‘black nerve’) against the high signal parotid parenchyma (‘white parotid’). Unfortunately, it is difficult to distinguish it from vessels, even in hyposignal, requiring a precise analysis of their respective paths to differentiate them. This sequence seems adapted to benign tumors but not to malignant tumors in contact with which the nerve is no longer visualized. In this case, the use of gadolinium-based contrast agent (GBCA) further increases negative contrast and improves differentiation of nerve from tumor (19).
Tractography seems to give the best results for predicting the facial nerve path, the ROI placed on the stylomastoidien foramen allows only the facial nerve fibers and is the most applicable in current practice since it is associated with the sequences used to describe tumors with an acquisition time acceptable to patients (9 additional minutes).
There are, however, limitations to this technique, linked in particular to the many type of artefacts: magnetic susceptibility, field homogeneity, movement, flux, and swallowing (18).

A reset between sequences is mandatory since the diffusion sequences are the last to be performed, the patient may have moved between the beginning and the end of the exam. The facial nerve path reconstruction performed on the diffusion sequences can be shifted on the anatomical sequences in the absence of resetting, making the interpretation of its position over the tumor erroneous.

The post-treatment necessary to obtain high quality images is still not automated today, which generally requires a significant involvement of practitioners and technicians. The initial ROI's position on the foramen stylomastoidien is decisive for tracked signal quality and must be placed by an experienced radiologist or technician. A shifted ROI, even by a single millimeter, may be outside of nerve path and may not pull any fibers or even pull fibers that do not belong to the facial nerve.

Further technological advances in sensitivity and automation are likely to lead to greater clinical use.

The main limitations of our study are the small number of patients and the method for describing the nerve position. In order to improve the kappa coefficient it would be interesting to perform a study on a larger population and a more objective method of comparison, such as that of El Kininy et al (12) based on photographs. To reduce movement artefacts, we could imagine a non-invasive immobilizer system such as those performed for some stereotactic MRI scans (20).

Many surgeries involve the prognosis of a peripheral nerve and could benefit from a tractographic analysis in pre-operation as already done for the facial nerve in acoustic neuroma surgery (21)(10). We are thinking in particular of the trigeminal nerve, very well visualized on the TWI map and already studied (21), which could be evaluated preoperatively by tractography in Trousseau's neuralgia (22).

Conclusion:

The facial nerve tractography performed prior to a parotidectomy could be an interesting tool for the surgeon. Predicting the nerve path, its relationship to the tumor and possible anatomical variations could enable the surgeon to anticipate the surgical procedure, its difficulty and the risk for the facial nerve, ensuring moreover better patient's information about preservation of his facial function. The anatomical resolution of the tractography seems adequate for the dissection of the trunk and the main division but still has limitations in small caliber branches.

Tractography could be a valuable support for difficult extractions, surgical revisions or tumors which are very far from the nerve on tractography and which do not require a complete removal of the gland without nerve dissection, preventing the associated risk of complications.
It would be interesting to continue through larger studies, and in particular studies where the surgeon would be aware of the tractography result, to analyze information's influence on the operating time, the rate of facial paralysis, and the modification of the type of surgery planned before tractography.

Financial disclosure and acknowledgement:

The authors would like to thank the Neuromédia association and the Head and Neck pole of the University Hospital of Reims for its financial support.

The authors thank Dr Jonathan Attali for his help in MRI analysis.

Conflict of interest:

The authors declare no conflict of interest.

REFERENCES

1. Hugo NE, McKinney P, Griffith BH. Management of tumors of the parotid gland. Surg Clin North Am. févr 1973;53(1):10511.
2. Califano J, Eisele DW. Benign salivary gland neoplasms. Otolaryngol Clin North Am. oct 1999;32(5):86173.
3. Cracchiolo JR, Shaha AR. Parotidectomy for Parotid Cancer. Otolaryngol Clin North Am. avr 2016;49(2):41524.
4. Bradley PJ. Primary malignant parotid epithelial neoplasm: nodal metastases and management. Curr Opin Otolaryngol Head Neck Surg. avr 2015;23(2):918.
5. Kwak HH, Park HD, Youn KH, Hu KS, Koh KS, Han SH, et al. Branching patterns of the facial nerve and its communication with the auriculotemporal nerve. Surg Radiol Anat SRA. déc 2004;26(6):494500.
6. Bassereau G, Touyeras A, Heitzmann P, Dauphin D. [Exposure of the facial nerve in the masseteric region during parotid surgery. Technical aspects and value]. Ann Oto-Laryngol Chir Cervico Faciale Bull Soc Oto-Laryngol Hopitaux Paris. 1997;114(6):239‑42.
7. Gupta S, Mends F, Hagiwara M, Fatterpekar G, Roehm PC. Imaging the facial nerve: a contemporary review. Radiol Res Pract. 2013;2013:248039.
8. Tsuchiya K, Imai M, Tateishi H, Nitatori T, Fujikawa A, Takemoto S. Neurography of the spinal nerve roots by diffusion tensor scanning applying motion-probing gradients in six directions. Magn Reson Med Sci MRMS Off J Jpn Soc Magn Reson Med. 2007;6(1):1‑5.
9. Haakma W, Hendrikse J, Uhrenholt L, Leemans A, Warner Thorup Boel L, Pedersen M, et al. Multicenter reproducibility study of diffusion MRI and fiber tractography of the lumbosacral nerves. J Magn Reson Imaging JMRI. 9 févr 2018;
10. Savardekar AR, Patra DP, Thakur JD, Narayan V, Mohammed N, Bollam P, et al.

Preoperative diffusion tensor imaging-fiber tracking for facial nerve identification in vestibular schwannoma: a systematic review on its evolution and current status with a pooled data analysis of surgical concordance rates. Neurosurg Focus. 2018;44(3):E5.
11. Attyé A, Karkas A, Troprès I, Roustit M, Kastler A, Bettega G, et al. Parotid gland tumours: MR tractography to assess contact with the facial nerve. Eur Radiol. juill 2016;26(7):2233‑41.
12. El Kininy W, Roddy D, Davy S, Roman E, O'Keane V, O'Hanlon E, et al. Magnetic resonance diffusion weighted imaging using constrained spherical deconvolution-based tractography of the extracranial course of the facial nerve. Oral Surg Oral Med Oral Pathol Oral Radiol. 5 févr 2020;
13. Andersson JLR, Skare S, Ashburner J. How to correct susceptibility distortions in spin-echo echo-planar images: application to diffusion tensor imaging. NeuroImage. oct 2003;20(2):870‑88.
14. Rouchy R-C, Attyé A, Medici M, Renard F, Kastler A, Grand S, et al. Facial nerve tractography: A new tool for the detection of perineural spread in parotid cancers. Eur Radiol. 9 avr 2018;
15. Calamante F. Track-weighted imaging methods: extracting information from a streamlines tractogram. Magma N Y N. août 2017;30(4):317‑35.
16. Attyé A, Karkas A, Troprès I, Roustit M, Kastler A, Bettega G, et al. Parotid gland tumours: MR tractography to assess contact with the facial nerve. Eur Radiol. juill 2016;26(7):2233‑41.
17. Tournier J-D, Calamante F, Connelly A. Determination of the appropriate b value and number of gradient directions for high-angular-resolution diffusion-weighted imaging. NMR Biomed. déc 2013;26(12):1775‑86.
18. Qin Y, Zhang J, Li P, Wang Y. 3D double-echo steady-state with water excitation MR imaging of the intraparotid facial nerve at 1.5T: a pilot study. AJNR Am J Neuroradiol. août 2011;32(7):1167‑72.
19. Bray TJ, Lim EA, Jawad S, Kaur S, Otero S, Beale TJ, et al. Negative-contrast neurography: Imaging the extracranial facial nerve and its branches using contrast-enhanced variable flip angle turbo spin echo MRI [Internet]. arXiv; 2021
20. Debus J, Essig M, Schad LR, Wenz F, Baudendistel K, Knopp MV, et al. Functional magnetic resonance imaging in a stereotactic setup. Magn Reson Imaging. 1996;14(9):1007‑12.
21. Borkar SA, Garg A, Mankotia DS, Joseph SL, Suri A, Kumar R, et al. Prediction of facial nerve position in large vestibular schwannomas using diffusion tensor imaging tractography and its intraoperative correlation. Neurol India. oct 2016;64(5):965‑70.
22. Xie G, Zhang F, Leung L, Mooney MA, Epprecht L, Norton I, et al. Anatomical assessment of trigeminal nerve tractography using diffusion MRI: A comparison of acquisition b-values and single- and multi-fiber tracking strategies. NeuroImage Clin. 2020;25:102160.
23. Lee C-C, Chong ST, Chen C-J, Hung S-C, Yang H-C, Lin C-J, et al. The timing of stereotactic radiosurgery for medically refractory trigeminal neuralgia: the evidence from diffusion tractography images. Acta Neurochir (Wien). 2018;160(5):977‑86.

Figure 1

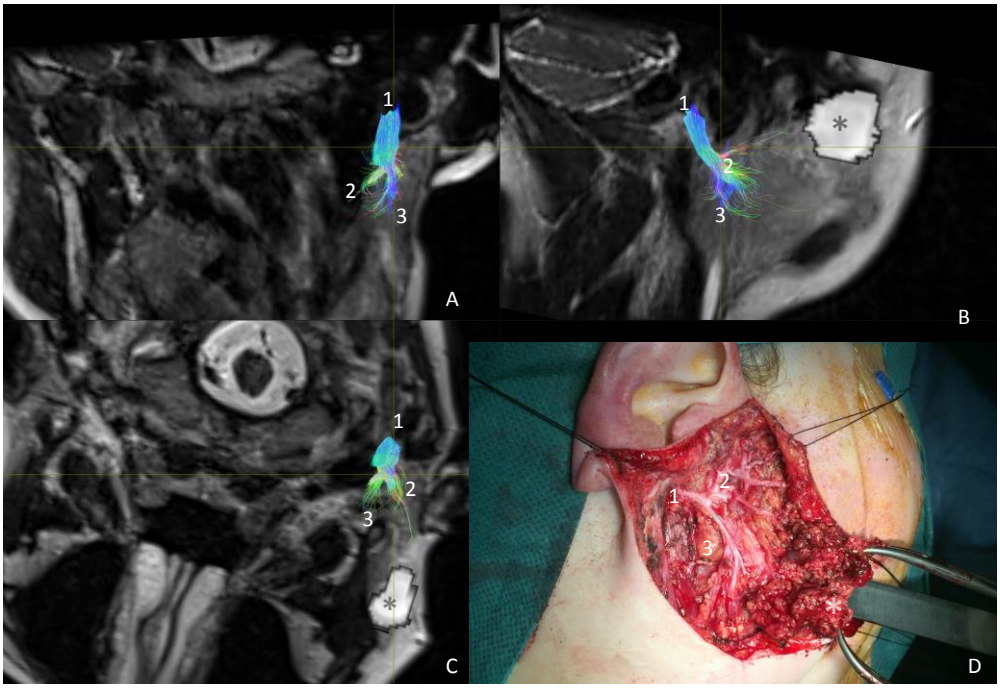

*Figure 1: Intra-parotid facial nerve, MRI tractography and surgery (modified slice plane for visualization of both nerve and mass). A: Coronal section. B: sagittal section. C: axial section. D: surgical view. *mass, 1=trunk, 2 = temporo-facial branch, 3 = cervicofacial branch, arrow = direction of dissection.*

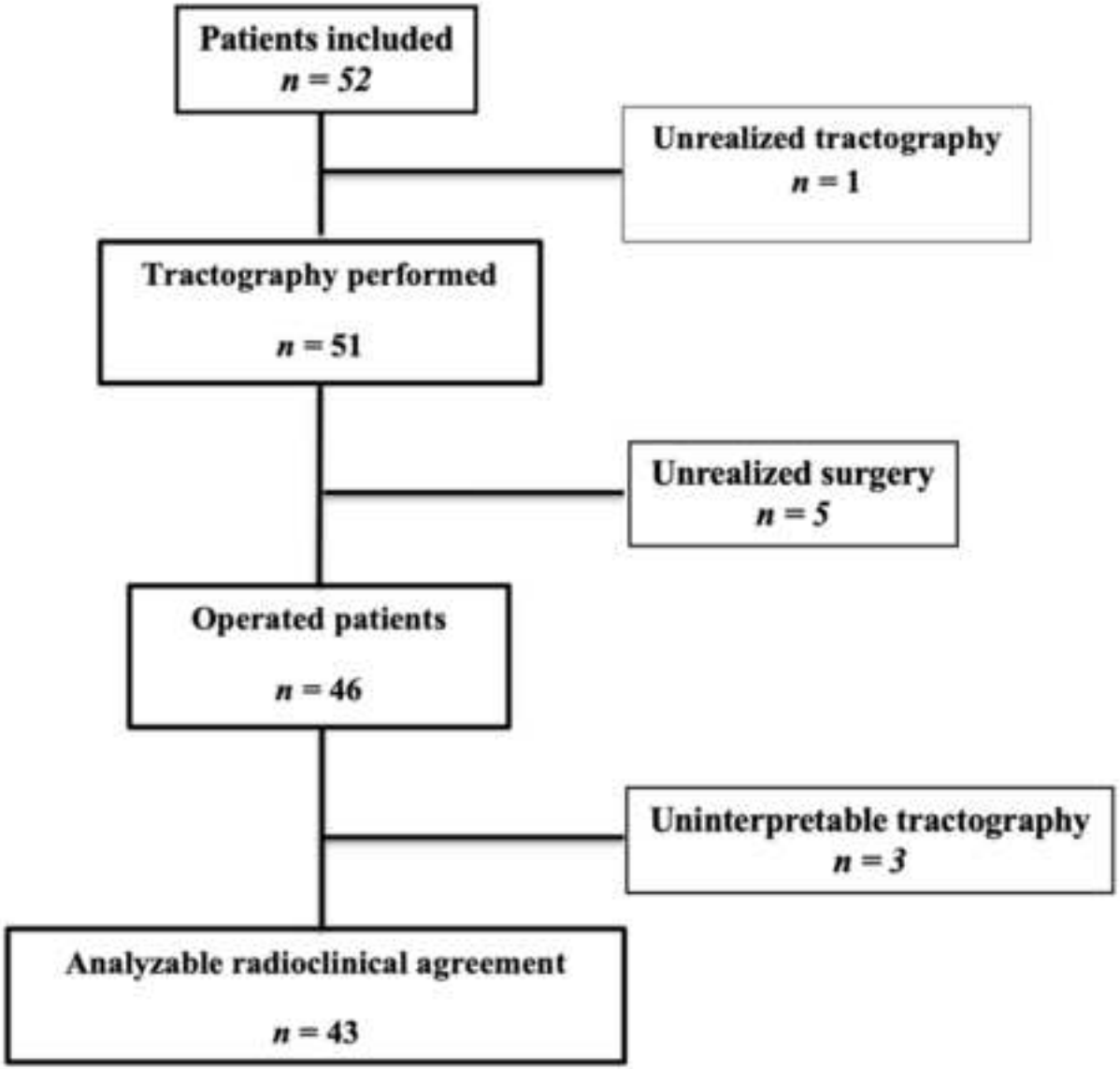

Table 1: Clinical patient's characteristics at inclusion

Characteristics	Value
Patients	
Age at inclusion (year) – Mean ± SD[1]	56±16
Sex ratio (F/M)	22 (47,8) /24 (52,2)
Homolateral antecedent of parotid surgery	4 (8,7)
Diabetes	6(13)
Neuropathy	1(1)
Tumor	
Side	
Right	22 (47,8)
Left	24 (52,2)
Symptoms	
Preoperative facial palsy	0
Presence of lymphadenopathy	1 (2,2)
Pain	2 (4,3)

Data are presented as n (%) unless otherwise indicated,
[1]Standard deviation

Table 2: Histopathologic characteristics, and surgery

Characteristics		Value
Surgery		
Type of parotidectomy		
Polar		5(10,87)
Exofacial		21(45,65)
Total		21 (45,65)
Cervical lymph node dissection		4 (8,70)
Facial nerve sacrifice		1 (2,17)
Post-operative facial palsy		14 (30,43)
Histology		
Definitive histopatology		
Tumor size (mm) – Mean ± SD[1]		26±17
Histological type		
Benign		35 (76,09)
	Pleomorphic Adenoma	17 (36,95)
	Cystadenolyphoma	12 (26,67)
	Salivary cyst	2 (4,44)
	Epidermal cyst	3 (6,52)
	Oncocytoma	1 (1,22)
	Schwannoma	1 (1,22)
		10 (21,74)
Malignant		
	Cystic adenoid carcinoma	2 (4,44)
	Mucoepidermoid carcinoma	2 (4,44)
	Canal adenocarcinoma	2 (4,44)
	Basal cell carcinoma	1 (2,22)
	Breast salivary carcinoma like	1 (2,22)
	Skin carcinoma metastasis	2 (4 ,44)
Perineural invasion		5 (10,87)
R status		
	R0	38 (82,61)
	R1	8 (17,39)

Data are presented as n (%) unless otherwise indicated, [1]Standard deviation

Table 3 revised

Table 3: Description of the nerve's position relative to the tumor visualized by MRI tractography, during surgery and radioclinic agreement.

	MRI[1]	Surgery	Data with agreement between radiologists and surgeon	K[2]
Trunk				
Visualized	43 (93,48)	43 (93,48)	-	-
Type of division				
Bifurcation	43 (100)	32 (82,05)	-	-
Trifurcation	0	7 (17,95)	-	-
Relative to the tumor				
Forward	1 (2,33)	1 (2,38)	36 (92,30)	0,37 [-0,18 ; 0,92]
Back	41 (95,34)	38 (90,48)		
On the frontal plane	1 (2,33)	3 (7,14)		
Below	2 (4,76)	5 (11,90)	26 (66,66)	0,36 [0,12 ; 0,60]
Above	30 (71,43)	21 (50,00)		
On the axial plane	10 (23,81)	16 (38,10)		
Inside	42 (97,77)	36 (85,71)	35 (89,74)	*
Outside	0	4 (9,52)		
On the sagittal plane	1 (2,33)	2 (4,76)		
Far>1cm	36 (83,72)	39 (92,85)	34 (85)	0,49 [0,10 ; 0,87]
Close<1 cm	6 (14,28)	3 (7,14)		
Temporal branch				
Visualized	**43 (93,48)**	**43 (93,48)**	-	-
Cartography				
Number of divisions± SD[3]	1 ±0,28	1±0,77	-	-
Number of endings± SD[3]	2,16 ±0,37	2,66±0,81	-	-
Relative to the tumor				
Forward	1 (2,38)	1 (2,38)	25 (65,79)	0,29 [0,02 ;0,56]
Back	32 (76,19)	23 (54,76)		
On the frontal plane	9 (21,43)	18 (42,86)		
Below	6 (13,95)	4 (9,52)	26 (66,66)	0,37 [0,13 ;0,62]
Above	27 (62,79)	23 (54,76)		
On the axial plane	10 (23,26)	15 (35,72)		
Inside	39 (90,70)	36 (83,72)	36 (90)	0,56 [0,17 ;0,94]
Outside	2 (4,65)	4 (9,30)		
On the sagittal plane	2 (4,65)	3 (6,98)		
Far>1cm	31 (73,81)	35 (81,40)	34 (84,5)	0,61 [0,34 ; 0,89]
Close<1 cm	11 (26,19)	8 (18,60)		
Cervicofacial branch				
Visualized	**43 (93,48)**	**42 (91,30)**	-	-
Cartography				
Number of divisions± SD[3]	1±0,24	1,2±0,61	-	-
Number of endings± SD[3]	2±0,33	2,44±0,90	-	-
Relative to the tumor				
Forward	2 (4,65)	1 (2,39)	27 (69,23)	*
Back	32 (74,42)	25 (60,98)		
On the frontal plane	9 (20,93)	15 (36,59)		
Below	9 (20,93)	11 (26,83)	25 (64,1)	0,42 [0,19 ; 0,65]
Above	13 (30,23)	9 (21,95)		
On the axial plane	21 (48 ,84)	21 (51,22)	36 (92,31)	0,64 [0,27 ; 1]
Inside	40 (93,02)	34 (82,93)		
Outside	1 (2,33)	4 (9,76)		
On the sagittal plane	2 (4,65)	3 (7,32)	30 (75)	0,52 [0,26 ; 0,78]
Far>1cm	24 (57,14)	21 (48,84)		
Close<1 cm	18 (42,86)	22 (51,16)		
Plane of division				
Visualized	**43 (95,56)**	**43 (93,48)**	-	-
Relative to the tumor				
Inside	39 (90 ,70)	35 (81,40)	34 (85)	0,35 [-0,04 ; 0,74]
Outside	1 (2,33)	6 (13,95)		

On the sagittal plane	2 (5,00)	2 (4,65)		
Far>1cm	9 (21,43)	10 (23,25)	31 (77,5)	0,26 [-0,1 ; 0,62]
Close<1 cm	33 (78,57)	33 (76,75)		
Frontal terminal branch				
Visualized	**23 (51,11)**	**33 (71,74)**	-	-
Relative to the tumor				
Forward	8 (38,10)	5 (15,62)	10 (55,55)	0,10 [-0,27 ; 0,48]
Back	2 (9 ,52)	4 (12,50)		
On the frontal plane	11 (52,38)	23 (71, 88)		
Below	2 (8,70)	0	15 (70)	*
Above	19 (82,61)	24 (100)		
On the axial plane	2 (8,70)	8 (25,00)		
Inside	20 (86,96)	28 (84,85)	18 (85,71)	0,50 [0,02 ; 0,99]
Outside	2 (8,70)	3 (9,09)		
On the sagittal plane	1 (4,34)	2 (6,06)		
Far>1cm	17 (73,91)	25 (78,13)	18 (85,72)	0,63 [0,25 ; 1]
Close<1 cm	6 (26,09)	7 (21,87)		
Eye's terminal branch				
Visualized	**23 (51,11)**	**34 (73,91)**	-	-
Relative to the tumor				
Forward	6 (26,09)	7 (21,21)	15 (71,42)	0,35 [0,02 ; 0,68]
Back	3 (13,04)	2 (6 ,06)		
On the frontal plane	14 (60,87)	24 (72,73)		
Below	1 (4,35)	3 (9,09)	14 (66,67)	*
Above	17 (73,91)	19 (57,58)		
On the axial plane	5 (21,74)	11 (33,33)		
Inside	21 (91,30)	28(82,36)	19 (86,37)	0,52 [0,08 ; 0,97]
Outside	1 (4,35)	3 (8,82)		
On the sagittal plane	1 (4,35)	3 (8,82)		
Far>1cm	10 (43,48)	19 (55,88)	19 (86,36)	0,73 [0,46 ; 1]
Close<1 cm	13 (56,52)	15 (44,12)		
Buccal terminal branch				
Visualized	**33 (73,33)**	**38 (82,61)**	-	-
Relative to the tumor				
Forward	7 (21 ,21)	9 (24,32)	22 (78,57)	*
Back	4 (12,12)	1 (2,71)		
On the frontal plane	22 (66,67)	27 (72,97)		
Below	9 (27,27)	12 (32,43)	14 (50)	0,26 [0,02 ; 0,52]
Above	13 (39,40)	7 (18,92)		
On the axial plane	11 (33,33)	18 (48,65)		
Inside	29 (87,88)	32 (86,49)	26 (99,66)	0,62 [0,23 ;1]
Outside	2 (6,06)	3 (8,11)		
On the sagittal plane	2 (6,06)	2 (5,40)		
Far>1cm	12 (36,36)	15 (40,54)	21 (72,41)	0,42 [0,07 ; 0,76]
Close<1 cm	21 (63,64)	22 (59,46)		
Mandibular terminal branch				
Visualized	**33 (73,33)**	**39 (84,78)**	-	-
Relative to the tumor				
Forward	4 (12,12)	10 (26,32)	18 (69,06)	0,22 [-0,05 ; 0,49]
Back	5 (15,15)	3 (7,89)		
On the frontal plane	24 (72,73)	25 (65,79)		
Below	16 (48,48)	22 (59,46)	17 (60,71)	*
Above	5 (15,16)	0		
On the axial plane	12(36,36)	15 (40,54)		
Inside	30 (90,91)	33 (89,18)	28 (96,56)	0,83 [0,54 ; 1]
Outside	1 (3,03)	2 (5,41)		
On the sagittal plane	2 (6,06)	2 (5,41)		
Far>1cm	15 (46,87)	18 (64,29)	18 (60)	0,21 [-0,15 ; 0,57]
Close<1 cm	17 (53,13)	20 (35,71)		

Data presented as n (%), [1]Magnetic Resonance Imagery : observations made by the two radiologists, [2]kappa: agreement coefficient between radiologists and surgeon findings [Confidence interval at 95%], [3]Standard deviation, * Kappa cannot be calculated because not the same response methods.

Full English Proofreading certificate